Study of Cl⁻(H₂O)ₙ (n = 1–4) Using Basin-Hopping Method Coupled with Density Functional Theory

Shuai Jiang,[a] Yi-Rong Liu,[a] Teng Huang,[a] Hui Wen,[a] Kang-Ming Xu,[a] Wei-Xiong Zhao,[a] Wei-Jun Zhang,[a,b] and Wei Huang*[a,b]

Cl⁻(H₂O)ₙ (n = 1–4) clusters were investigated using a basin-hopping (BH) algorithm coupled with density functional theory (DFT). Structures, energetics, thermodynamics, vertical detachment energies, and vibrational frequencies were obtained from high-level *ab initio* calculations. Through comparisons with previous theoretical and experimental data, it was demonstrated that the combination of the BH method and DFT could accurately predict the global and local minima of Cl⁻(H₂O)ₙ (n = 1–4). Additionally, to optimize larger Cl⁻(H₂O)ₙ (n > 4) clusters, several popular density functionals as well as

DF-LMP2 (Schütz et al., J. Chem. Phys. 2004, 121, 737) (second-order Møller-Plesset perturbation theory using local and density fitting approximations) were tested with appropriate basis sets through comparisons with MP2 optimized results. DF-LMP2 will be used in future studies because its overall performance in describing the relative binding energies and the geometrical parameters of Cl⁻(H₂O)ₙ (n = 1–4) was outstanding in this study. © 2013 Wiley Periodicals, Inc.

Introduction

Halide-water clusters are very important in cluster science because they have unique thermodynamic and spectroscopic properties. Other studies have focused on the following aspects of halide-water clusters: structures,[1,2] thermodynamics,[3,4] vibrational spectroscopy,[5–8] photoelectron spectroscopy (PES)[9] and charge-transfer-to-solvent (CTTS) energies.[10,11] In particular, the experimental work of Johnson and coworkers,[5,6,8] Okumura and coworkers,[7] and Cheshnovsky and coworkers[9] provided a great deal of spectroscopic data that yielded critical structural information. Theoretical studies by Kim et al.[1,12,13] applied high-level *ab initio* calculations to determine structures of many halide-water clusters.

In many calculations, manual searches are performed to obtain information about potential energy surface minima. This approach is less reliable for larger molecular systems with enormous minima, which has motivated the use of many global optimization techniques such as Genetic algorithms (GAs),[14–16] Monte Carlo (MC) simulated annealing,[17] minima hopping,[18] and basin-hopping (BH).[19]

For halide-water systems, Neogi and Chaudhury[20,21] recently used GA coupled with density functional theory (DFT) to identify the local and the global minima. They demonstrated that this strategy based on GA and DFT is viable for investigating halide solvation systems.

In contrast, BH code has been coupled with quantum chemistry packages such as Dmol³[22] to search for the lowest energy isomers of atomic clusters. The BH approach is highly efficient for many atomic clusters, especially gold[23–26] and boron clusters.[27] Furthermore, the ability of BH algorithms coupled with DFT to search for minima on the potential energy surfaces of molecular clusters has been tested for water, methanol, and water + methanol clusters, protonated and unprotonated,[28] as well as the structure and the bonding in ionized water clusters.[29] To the

best of our knowledge, no research has been published on the ability of BH to search for the lowest energy isomers of halide solvation clusters, and it is necessary to examine the further optimization of BH for larger halide solvation systems.

In this study, BH was coupled with DFT and used to determine the local and global minima of chloride-water clusters. The structures of Cl⁻(H₂O)ₙ, Br⁻(H₂O)ₙ, and I⁻(H₂O)ₙ clusters[1] are similar, and only chloride-water clusters were investigated to reduce computational costs. Because the structural characteristics of F⁻(H₂O)ₙ are quite different from those of other halide solvation clusters,[1] we did not include fluoride-water clusters in this study. This article presents the structures, energetics, thermodynamics, vertical detachment energies (VDEs), and vibrational frequencies of Cl⁻(H₂O)ₙ (n = 1–4) clusters. Additionally, several popular density functionals and DF-LMP2 were evaluated for optimizing larger chloride-water clusters to provide guidance on selecting computational methods.

Methodology

The potential energy surfaces of Cl⁻(H₂O)ₙ (n = 1–4) were explored with the BH algorithm coupled with DFT implemented in Dmol³.[22] The number of BH searches ranged from 2 to 5

[a] S. Jiang, Y.-R Liu, T. Huang, H. Wen, K.-M Xu, W.-X Zhao, W.-J Zhang, W. Huang
Laboratory of Atmospheric Physico-Chemistry, Anhui Institute of Optics and Fine Mechanics, Chinese Academy of Sciences, Hefei, Anhui 230031, China
E-mail: huangwei6@ustc.edu.cn

[b] W.-J Zhang, W. Huang
School of Environmental Science and Optoelectronic Technology, University of Science and Technology of China, Hefei, Anhui 230026, China

according to the cluster size. Every search was performed with 1000 MC steps at 2000 K with randomly generated initial structures. The temperature is a crucial parameter in BH, and the temperature must be chosen carefully because it affects the tradeoff between the acceptance ratio and the sampling efficiency. At each MC step, all of the molecules were translated and rotated, and the maximum translational and rotational displacements were 2 Å and $\pi/2$, respectively. To prevent the divergence of the clusters, we compiled a function to check whether the intermolecular distances exceeded the range defined after the structure perturbation caused by the MC sampling. After each MC step, this function automatically determined whether the molecule moved more than 5 Å, which could cause the optimization to fail. If a large divergence occurred, then this function automatically moved the molecules closer together. The atoms in different molecules were not permitted to be closer than 2 Å to prevent the self-consistent field calculation from failing to converge.

In Dmol[3],[22] there were two steps in the optimization procedure: the first optimization step was at the BLYP/DND level, where BLYP means Becke for the exchange part and Lee, Yang and Parr for the correlation part and DND means double numerical plus d-functions basis set and the second optimization step was at the BLYP/DNP level, in which DND represents double numerical plus polarization basis set. Next, these twice-optimized structures were optimized again using the Gaussian09 suite of programs[30] by MP2/aug'-cc-pVDZ, where the prime signified that aug-cc-pVDZ was used for Cl and O and cc-pVDZ was used for H. The default convergence criteria were defined in the Gaussian09 suite of programs.[30] Harmonic vibrational frequency analysis was performed to verify that no imaginary frequencies were present and, consequently, the structure of interest represented a local or a global minimum on the potential energy surface. The zero-point energy (ZPE), the enthalpy and the Gibbs free energy corrections were obtained at 1 atm and 298 K. The basis set superposition error (BSSE) was calculated using the counterpoise correction (CP) method.[31] For $n = 4$, the vibrational frequencies and the thermodynamics calculations were carried out with Molpro 2010.1.[32,33] Based on the MP2/aug'-cc-pVDZ optimized geometries, single point energy calculations at the MP2/aug'-cc-pVTZ level were conducted to obtain the VDEs.

The performance of different density functional and *ab initio* methods in calculations of the structures and the energetics was investigated using the MP2/aug'-cc-pVDZ geometries. At the MP2/aug'-cc-pVTZ and the DF-LMP2/aug'-cc-pVTZ levels, the calculations were performed with Molpro 2010.1,[32,33] whereas the other calculations were carried out using density functionals with basis sets computed with the Gaussian09 suite of programs.[30] The relative binding energies, with and without the ZPE corrections, were given for clusters with up to four water molecules. Because only relative binding energies were offered, the BSSE was not performed. Additionally, the structural information (bond lengths) was provided through direct comparison, and the root-mean-squared distances (RMSD) were obtained with MP2/aug'-cc-pVTZ optimized structures in Chemcraft 1.6 (http://www.chemcraftprog.com).
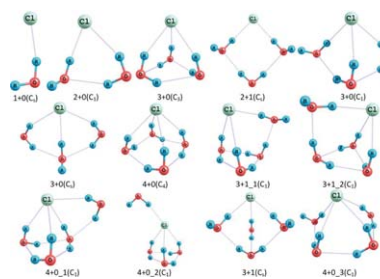

Figure 1. The global minimum and the local minima for Cl⁻(H2O)n (n = 1–4) optimized at the MP2/aug'-cc-pVDZ level. [Color figure can be viewed in the online issue, which is available at wileyonlinelibrary.com.]

To investigate the performance of these density functionals and DF-LMP2 in a more rigorous manner, it was necessary to directly compare the calculated and the experimental values of the enthalpy and the Gibbs binding energies. We carried out an additional geometry optimization for Cl⁻(H2O)n (n = 1–4) with CPs using the functionals that were based on BLYP/DNP optimized structures and comparable to the mp2/aug'-cc-pVDZ optimized structures. Because local methods are particularly useful for calculating the weak intermolecular interactions, as the BSSE is reduced significantly,[34,35] we simply used DF-LMP2/aug'-cc-pVDZ without CP corrections to optimize geometries. The enthalpy and the Gibbs free energy corrections from the mp2/aug'-cc-pVDZ frequency calculations were added to the electronic energies calculated with these methods. The global minima of the electronic energies of the Cl⁻(H2O)n (n = 1–4) clusters were selected for these comparisons.

Results and Discussion

Structures and energetics

The representations of these structures were defined using m + n_i() notation with the symmetry given in parentheses. In this notation, "m" and "n" denote the number of water molecules in the first and the second hydration shells of the clusters, respectively. The index "i" is used to distinguish different structures with the same values of m and n. This index was not used when only one structure existed for particular values of m and n.

An overview of all the structures suggests that the Cl⁻(H2O)n (n = 1–4) clusters prefer surface solvation, as discussed previously in the literature.[2]

Figure 1 shows the structures optimized with MP2/aug'-cc-pVDZ. In the global minimum of Cl⁻(H2O), a chloride ion bonds to one water molecular with a free OH group, whereas the global minimum of Cl⁻(H2O)2 has a free OH group. Both structures are in good agreement with structures optimized at the MP2/aug'-cc-pVDZ level by Xantheas.[36]

The minima of Cl⁻(H2O)3 includes the global minimum and a competing local minima with relative binding energies that are within 3 kcal mol⁻¹ (ZPE excluded). For the global minimum, the three water monomers form a ring that resembles the base of a pyramid with the halide anion at its apex. A significant structural difference is found between 2 + 1(C_s) and 3 + 0(C_1) where the latter structure has one additional bond with the chloride ion. However, the binding energy difference

Table 1. Binding energies ($-\Delta E_e$), BSSE-corrected energies ($-\Delta E_e^B$), ZPE-corrected energies ($-\Delta E_0$), BSSE-corrected and ZPE-corrected energies ($-\Delta E_0^B$) at 0 K, enthalpies ($-\Delta H$), BSSE-corrected enthalpies ($-\Delta H^B$), Gibbs free energy ($-\Delta G$), and BSSE-corrected Gibbs free energies ($-\Delta G^B$) at 298 K and 1 atm for various isomers of $Cl^-(H_2O)_n$ ($n = 1$–4) and the experimental enthalpies ($-\Delta H_{exp}$) and Gibbs free energies ($-\Delta G_{exp}$) (in kcal mol^{-1})

n	Isomers	$-\Delta E_e(-\Delta E_e^B)$	$-\Delta E_0(-\Delta E_0^B)$	$-\Delta H(-\Delta H^B)$	$-\Delta G(-\Delta G^B)$	$-\Delta H_{exp}$[a]	$-\Delta G_{exp}$[a]
1	$1 + 0(C_s)$	14.2(13.7)	13.0(12.5)	13.8(13.3)	7.8 (7.2)	14.7, 13.1	8.8, 8.2
2	$2 + 0(C_1)$	28.7(27.3)	25.1(23.7)	26.6(25.2)	11.7(10.3)	27.7, 25.8	15.4, 14.7
3	$3 + 0(C_3)$	44.0(41.4)	37.3(34.7)	39.8(37.1)	14.4(11.8)	39.5, 37.5	20.6, 19.2
	$2 + 1(C_s)$	41.9(39.5)	36.1(33.7)	38.2(35.8)	14.3(11.9)		
	$3 + 0(C_1)$	41.9(39.6)	36.0(33.7)	38.0(35.7)	14.1(11.8)		
	$3 + 0(C_s)$	41.2(39.0)	35.6(33.4)	37.5(35.3)	14.5(12.3)		
4	$4 + 0(C_4)$	58.0(53.9)	48.6(44.4)	51.8(47.7)	16.2(12.1)	50.1, 48.6	24.4, 22.6
	$3 + 1\_1(C_1)$	56.9(53.0)	47.9(44.0)	51.6(47.7)	14.9(11.0)		
	$3 + 1\_2(C_1)$	56.8(52.9)	47.8(43.9)	51.5(47.6)	14.8(10.9)		
	$4 + 0\_1(C_1)$	55.4(51.8)	47.0(43.4)	50.3(46.7)	14.7(11.1)		
	$4 + 0\_2(C_1)$	54.5(51.3)	46.8(43.6)	50.8(47.6)	13.6(10.4)		
	$3 + 1(C_s)$	54.3(50.8)	46.3(42.7)	50.0(46.5)	13.2(9.6)		
	$4 + 0\_3(C_1)$	53.9(50.5)	46.0(42.6)	49.6(46.2)	13.2(9.8)		

[a] The first and second of experimentally predicted—and—are from Hiraoka et al.[4] and Arshadi et al.,[3] repectively.

between these two structures is negligible (within 0.1 kcal mol^{-1}) even when ZPE is included.

It is not unusual to encounter various isomers for a particular value of n because different isomers can be produced by merely changing the hydrogen bond orientation of the water "ring." The global minimum of $Cl^-(H_2O)_4$ has a pyramidal structure similar to the global minimum of $Cl^-(H_2O)_3$, but the base of $Cl^-(H_2O)_4$ is a "ring" of four instead of three water molecules. The binding energy difference between the global minimum and the nearest local minimum is only 1.1 kcal mol^{-1} less than in the case of $Cl^-(H_2O)_3$. This binding energy difference indicates that the energy difference among minima on the potential surface is decreasing. The $3 + 1\_1(C_1)$ and $3 + 1\_2(C_1)$ structures are isoenergetic for binding energies with and without ZPE because the only significant structural difference is the orientation of the water-ring in the base, which has little influence on the energetics.

Thermodynamics

The calculated and the experimental thermodynamic parameters are given in Table 1. The experimental values from Arshadi et al.[3] are underestimated systematically relative to those from Hiraoka et al.[4] The theoretically predicted thermodynamic values are in good agreement with the experimental values. However, there is less agreement between the theoretical BSSE-corrected Gibbs free energy changes and the experimental values from Arshadi et al.[3] and Hiraoka et al.[4] than for the enthalpy values. The BSSE-corrected enthalpy and the Gibbs free energy changes are theoretically more rigorous. However, the BSSE-free Gibbs free energies are closer to the experimental values. As the number of water molecules in the solvation cluster increases, the extent of agreement with experimental data decreases, indicating that more structures are competing with the global minimum.

VDEs

The experimental VDEs have been given by the photoelectron spectroscopy (PES) experiment by Cheshnovsky's group.[9] The

experimental peak widths are the consequence of the deviations of the ionic and molecular states from equilibrium geometries and the contributions from the various isomers.

Our simulations predicted the VDEs of various isomers shown in Table 2, including those of the global minimum and many local minima. There is very good agreement between the theoretical and the experimental values of the VDEs. However, the PES is regarded only as a necessary condition to confirm the rationality of the structures, which indicates that the global minimum cannot be distinguished from the local minima through the PES alone. Consequently, the IR spectra provide essential structural information about the arrangement of water molecules around the chloride anion.

Vibrational frequencies

Table 3 gives the O—H frequencies of $Cl^-(H_2O)_n$ ($n = 1$–4) from both experimentally and theoretically predicted IR spectra. The O—H stretching frequencies of chloride-water clusters are classified as follows: (1) nonbonded free[(O—H_f)], (2) hydrogen bonded to another water [(O—H_w)], and (3) hydrogen

Table 2. Experimental and calculated (at MP2/aug'-cc-pVTZ level) values [in electron volts (eV) units] of the first vertical detachment energies (VDEs) of the major isomers of $Cl^-(H_2O)_n$ ($n = 1$–4) (in eV).

n	Isomers	VDE$_{theor}$	VDE$_{exp}$[a]
1	$1 + 0(C_s)$	4.33	4.37
2	$2 + 0(C_1)$	4.94	4.97
3	$3 + 0(C_3)$	5.49	5.50
	$2 + 1(C_s)$	5.41	
	$3 + 0(C_1)$	5.50	
	$3 + 0(C_s)$	5.50	
4	$4 + 0(C_4)$	5.84	5.92
	$3 + 1\_1(C_1)$	5.83	
	$3 + 1\_2(C_1)$	5.82	
	$4 + 0\_1(C_1)$	5.99	
	$4 + 0\_2(C_1)$	5.99	
	$3 + 1(C_s)$	5.85	
	$4 + 0\_3(C_1)$	5.95	

[a] Experimental VDEs are from Ref. [10].

Table 3. Simulated[a] and experimentally predicted vibrational frequencies for $Cl^-(H_2O)_n$ (n = 1–4) (in)

n	Isomers	ω (O—Hx)	ω (O—Hw)	ω (O—Hf)	exp
1	1 + 0(C_s)	3195		3625	3130, 3690[b]
2	2 + 0(C_1)	3162, 3387	3550	3617	3130, 3375, 3633, 3686[b]
3	3 + 0(C_3)	3343, 3346, 3367	3514, 3525, 3526		3310, 3354, 3391
	2 + 1(C_s)	3172, 3205	3418, 3251	3617, 3618	3585, 3600[b]
	3 + 0(C_1)	3205, 3366, 3433	3525, 3541	3616	
	3 + 0(C_s)	2996, 3422, 3430	3563, 3569	3614	
4	4 + 0(C_4)	3370, 3379, 3380, 3388	3454, 3455,3458, 3461		3408, 3590, 3694[c]
	3 + 1_1(C_1)	3134, 3321, 3367	3346, 3435, 3458, 3520	3618	
	3 + 1_2(C_1)	3127, 3328, 3372	3351, 3434, 3468, 3498	3621	
	4 + 0_1(C_1)	3302, 3341, 3389, 3442	3484, 3500, 3550, 3562		
	4 + 0_2(C_1)	3341, 3368, 3378, 3402	3489, 3499, 3503	3633	
	3 + 1(C_s)	3139, 3176	3371, 3427, 3448, 3509	3624, 3626	
	4 + 0_3(C_1)	3233, 3384, 3395, 3454	3508, 3513, 3533	3622	

[a] Simulated vibrational frequencies scaled by 0.93. [b] Those experimental IR data are from Johnson group.[5,6,8] [c] Those experimental IR data are from Okumura group.[8]

bonded to a chloride atom [(O—H$_x$)], as shown in Table 3. Considering the large red shifts for ionic hydrogen bonds (IHB), an IHB is strengthened at the expense of weakening of the hydrogen bonding between water molecules. Overall, the free O—H stretching frequencies remain almost constant with respect to the corresponding mean of the symmetric and asymmetric OH stretches in water (3882 cm^{-1}). Thus, the elongation of an IHB contributes considerably to their large red shifts. Similarly, red shifts are much smaller in magnitude for the hydrogen-bonded O—H frequencies than the IHBs.

Our simulated vibrational frequencies are consistent with the experimental results from Johnson and coworkers[5,6,8] and Okumura and coworkers.[7] The frequencies from our theoretical predictions are slightly blue shifted relative to the experimental frequencies. This blue shift can be attributed to the harmonic approximation used in the frequency calculation. The scaling factor of 0.93, which was recommended by Neogi and Chaudhury,[20] is useful for matching the major peaks in experimental data.

Density functionals and DF-LMP2 testing

Several density functionals and DF-LMP2 were tested for optimizing larger molecular systems. Additionally, several methods were used to investigate the potential energy surfaces and observe the flatness when ZPE is included in the calculations.

Instead of testing dozens of density functionals, which was very time-consuming, we selected several density functionals and DF-LMP2 on the basis of their outstanding performance, especially in describing the hydrogen bonds in water clusters.

B3LYP was chosen based on its widespread popularity. X3LYP was selected because Xu and Goddard[37] demonstrated that for binding energy evaluation, X3LYP outperformed a variety of density functionals in binding energy calculations of hydrogen-bonded systems such as water clusters. Additionally, they showed that X3LYP provides reliable geometrical parameters and relative energies for water dimers at the CCSD(T), indicating coupled-cluster singles, doubles, and triples level.[38] Li et al.[39] showed that X3LYP with the 6-311 + G(2df,2p) basis set predicted geometries of $(H_2O)_n$ (1–2) clusters that

were in good agreement with the experimental values, whereas X3LYP/6-31 + G(2d,p) gave satisfactory results. We also included the combination of B2PLYP hybrid DFT with semiempirical MP2 and B2PLYPD, which is B2PLYP with "D2" dispersion corrections.[40,41] The aug'-cc-pVTZ was chosen as the basis set for comparing with the MP2/aug'-cc-pVTZ optimized results. In the following discussion, the method will be mentioned without its basis set.

Figure 2 compares the relative binding energies of the structures that were optimized with the above methods and the structures that were optimized by the MP2 without ZPE corrections. The five tested methods did not change the energy ordering, but the various methods showed different levels of agreement with the MP2 optimized results. From the perspective of mean squared error (MSE) and root-mean-square error (RMSE), B2PLYP gave the best estimate while the X3LYP results
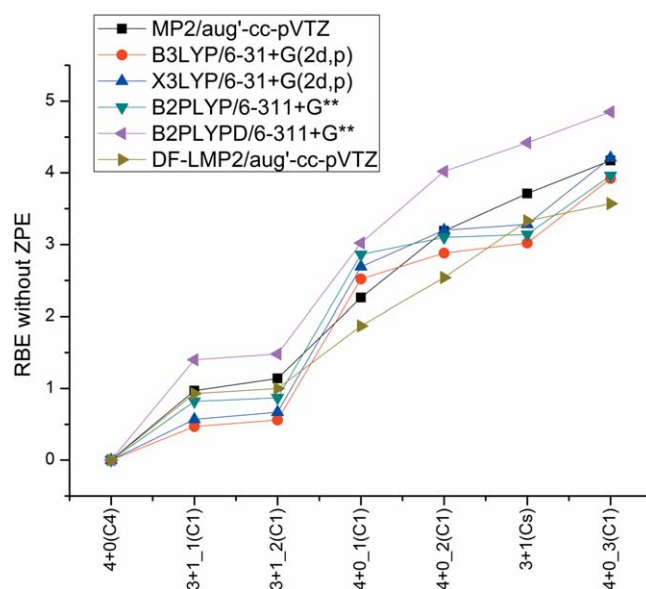

Figure 2. The relative binding energies (RBE) of test methods optimized structures compared with the MP2/aug'-cc-pVTZ optimized structures without zero-point energy (ZPE) corrections. [Color figure can be viewed in the online issue, which is available at wileyonlinelibrary.com.]
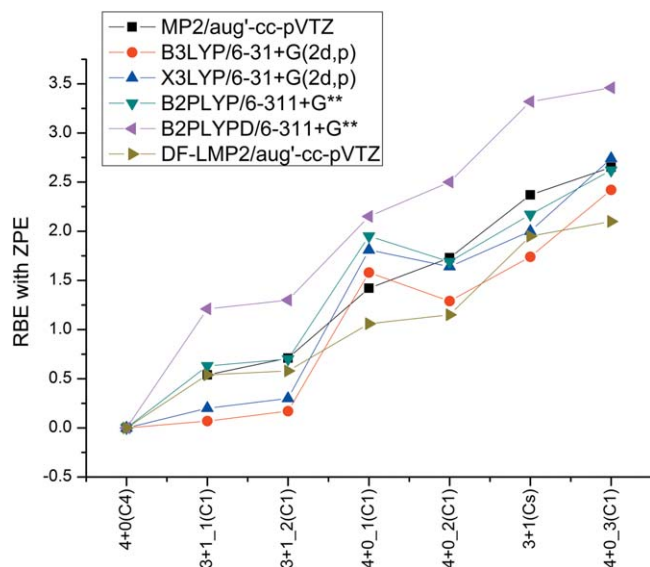
Figure 3. The relative binding energies (RBE) of test methods optimized structures compared with the MP2/aug'-cc-pVTZ optimized structures with zero-point energy (ZPE) corrections.

Figure 4. The average Cl—H hydrogen bond lengths (in Å) of structures optimized under tested methods.

were competitive. Additionally, DF-LMP2 systematically underestimated the relative binding energies while B2PLYPD systematically overestimated these energies, although DF-LMP2 was in better agreement with MP2.

Figure 3 illustrates the relative binding energies with ZPE for these methods. These results were consistent with those from Figure 2, as B2PLYP and X3LYP gave the best estimates from the comparison of MSE and RMSE values with those of MP2. B2PLYPD and DF-LMP2 showed the same systematic error trends, as shown in Figure 3. However, only B2PLYPD and DF-LMP2 gave the same energy ordering as MP2.

Figure 4 shows the average Cl—H hydrogen bond lengths for $Cl^-(H_2O)_n$ ($n = 1$–4). DF-LMP2 gave the best estimate of the average bond lengths, MSE and RMSE while the other four methods gave similar estimates. All the tested methods systematically overestimated the bond lengths between the chloride ion and the hydrogen atom, but DF-LMP2 gave the smallest overestimate.

The average O—H covalent bond lengths are given in Figure 5, which indicates the interactions inside the molecular clusters. All the tested methods showed systematic errors and were very similar, but DF-LMP2 still gave the best estimates of the average bond lengths.

The treatment of the O—H hydrogen bond is very important, indicating one aspect of weak interactions. As shown in Figure 6, B2PLYPD and DF-LMP2 are the only two methods that gave systematic discrepancies, similar to their treatment of the relative binding energies with ZPE. However, at this time, B2PLYPD gave better average bond lengths. X3LYP gave the best estimates of the MSE and the RMSE in spite of its inconsistency.

Figure 7 shows the RMSD values obtained by rotating and translating one of the structures to minimize its RMSD values. X3LYP gave the best estimates of the average RMSD values, but DF-LMP2 gave very low RMSD values in most cases except
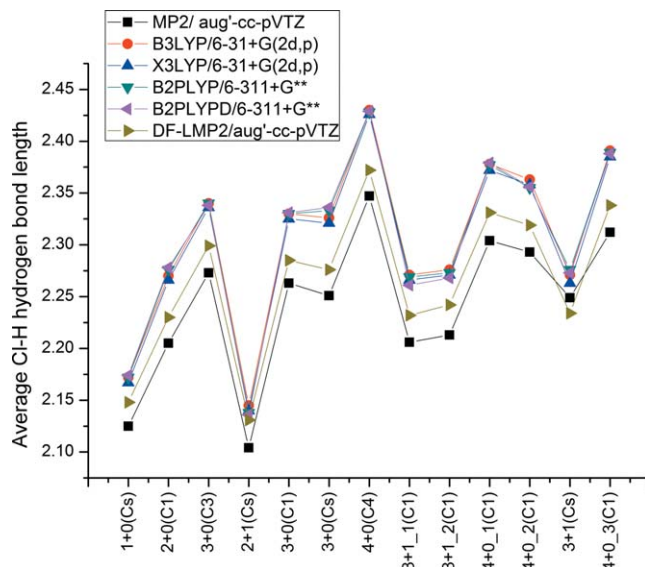
$3 + 0(C_s)$ and $4 + 0\_2(C_1)$. Despite these two unexpected results, DF-LMP2 provided a low average RMSD value of 0.060.

Overall, DF-LMP2 gave the best prediction of the structures and energetics for $Cl^-(H_2O)_n$ ($n = 1$–4) with good systematic behavior, even though X3LYP and B2PLYPD both showed good performance. However, the most popular density function—B3LYP did not show equally good performance.

To visualize the performance of the tested methods, we used the thermal values of the tested methods as well as the experimental values from Hiraoka's group[4] divided by the Arshadi group's experimental values,[3] shown in Figures 8 and 9.

As shown Figure 8, the tested methods showed various patterns, although their absolute differences were actually small, as the experimental maximum enthalpy values from Hiraoka's group[4] are 2.4 kcal mol^{-1}. The enthalpy values from B2PLYPD
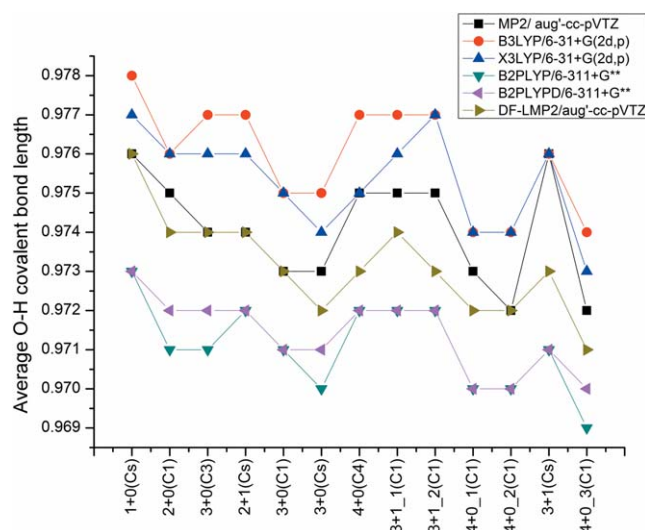

Figure 5. The average O—H covalent bond lengths (in Å) of structures optimized under tested methods. [Color figure can be viewed in the online issue, which is available at wileyonlinelibrary.com.]
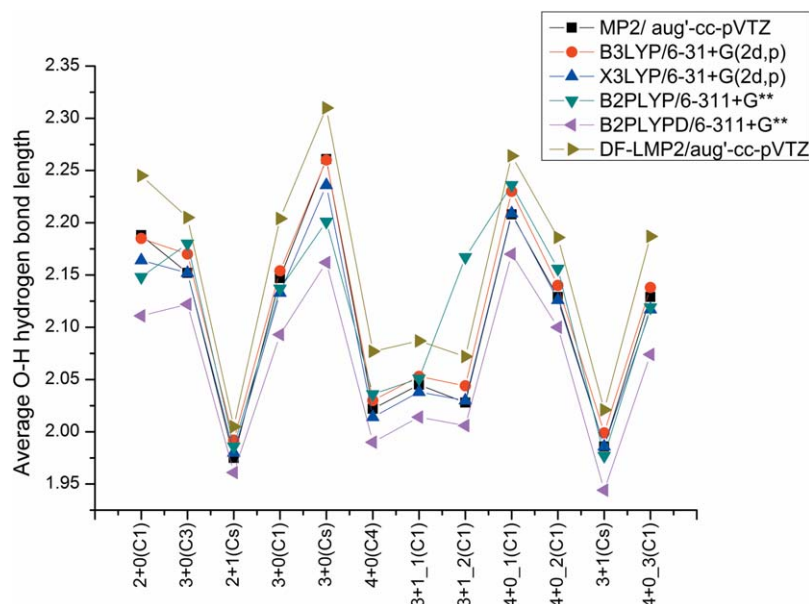
Figure 6. The average O—H hydrogen bond lengths (in Å) of structures optimized under tested methods. [Color figure can be viewed in the online issue, which is available at wileyonlinelibrary.com.]

and X3LYP approached the Hiraoka group's experimental values,[4] whereas the rest were close to the experimental results from Arshadi's group.[3] Considering these small absolute differences as well as the experimental uncertainty, it is unclear which method gave the best enthalpy corrections. However, the systematic behaviors indicated that B2PLYPD and X3LYP systematically overestimated the enthalpy corrections compared with the estimates of MP2 while the results did not systematically approach MP2 values.

The significant disagreement between the theoretical values from all the tested methods and the experimental results shown in Figure 9 indicates that the potential energy surfaces of $Cl^-(H_2O)_n$ (n = 1–4) systems are flat and local minima con-

tribute significantly to the Gibbs free energy, which explains why all the tested methods substantially underestimated the Gibbs free energy. These results were size dependent, and the gaps between the theoretical and the experimental values were larger for bigger systems. Although the B2PLYPD and the X3LYP results were closer to the experimental values, it is difficult to determine which method gave the most accurate Gibbs free energy corrections for $Cl^-(H_2O)_n$ systems, which have almost structureless potential energy surfaces.

Conclusions

In this article, the validity of using BH to search for the global and the local minima of $Cl^-(H_2O)_n$ (n = 1–4) was confirmed
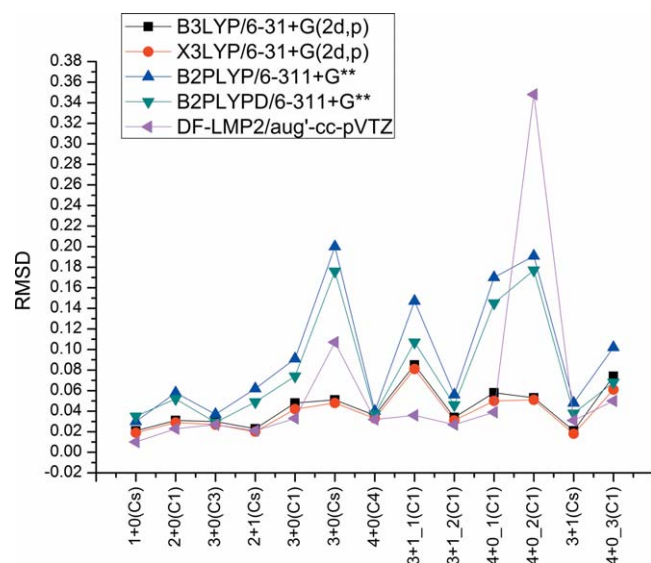

Figure 7. The RMSD (in Å), as compared with MP2/aug'-cc-pVTZ optimized structure. [Color figure can be viewed in the online issue, which is available at wileyonlinelibrary.com.]
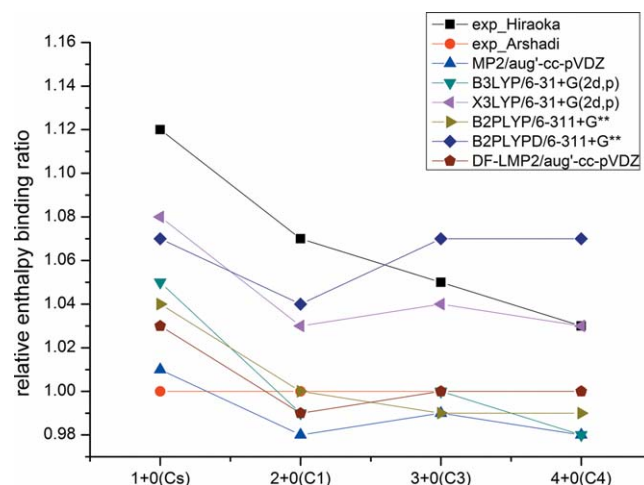

Figure 8. The relative enthalpy binding ratio for comparisons between tested methods and experimental values. [Color figure can be viewed in the online issue, which is available at wileyonlinelibrary.com.]
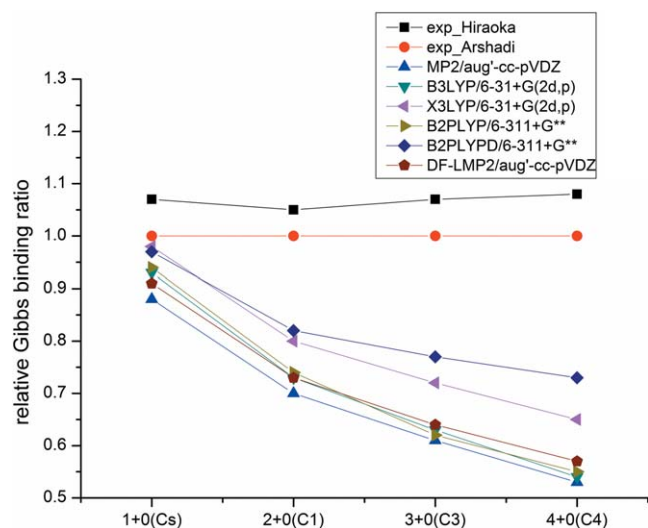
Figure 9. The relative Gibbs binding ratio for comparisons between tested methods and experimental values. [Color figure can be viewed in the online issue, which is available at wileyonlinelibrary.com.]

by comparing the theoretically predicted structures, energetics, thermodynamics, VDEs and vibrational frequencies with the experimentally determined values. The results from several popular density functional and DF-LMP2 methods contribute to choosing the most appropriate method to optimize larger $Cl^-(H_2O)_n$ ($n > 4$) clusters. Based on our results, the DF-LMP2 optimization approach coupled with BH will be used in the future to produce initial geometries for investigating the larger $Cl^-(H_2O)_n$ ($n > 4$) clusters. However, for calculating the thermal corrections, each of the tested functionals showed good performance, and none of these methods are strongly recommended as the best for $Cl^-(H_2O)_n$ systems.

[1] J. Kim, H. M. Lee, S. B. Suh, D. Majumdar, K. S. Kim, *J. Chem. Phys.* **2000**, *113*, 5259.

[2] R. W. Gora, S. Roszak, J. Leszczynski, *Chem. Phys. Lett.* **2000**, *325*, 7.

[3] M. Arshadi, R. Yamdagni, P. Kebarle, *J. Phys. Chem. A* **1970**, *74*, 1475.

[4] K. Hiraoka, S. Mizuse, S. Yamabe, *J. Phys. Chem. A* **1988**, *92*, 3943.

[5] P. Ayotte, G. H. Weddle, M. A. Johnson, *J. Chem. Phys.* **1999**, *110*, 7129.

[6] P. Ayotte, S. B. Nielsen, G. H. Weddle, M. A. Johnson, S. S. Xantheas, *J. Phys. Chem. A* **1999**, *103*, 10665.

[7] J.-H. Choi, K. T. Kuwata, Y.-B. Cao, M. Okumura, *J. Phys. Chem. A* **1998**, *102*, 503.

[8] P. Ayotte, G. H. Weddle, J. Kim, M. A. Johnson, *J. Am. Chem. Soc.* **1998**, *120*, 12361.

[9] G. Markovich, S. Pollack, R. Giniger, O. Cheshnovsky, *J. Chem. Phys.* **1994**, *101*, 9344.

[10] D. Serxner, C. E. H. Dessent, M. A. Johnson, *J. Chem. Phys.* **1996**, *105*, 7231.

[11] N. Takahashi, K. Sakai, H. Tanida, I. Watanabe, *Chem. Phys. Lett.* **1995**, *246*, 183.

[12] H. M. Lee, D. Kim, K. S. Kim, *J. Chem. Phys.* **2002**, *116*, 5509.

[13] H. M. Lee, K. S. Kim, *J. Chem. Phys.* **2001**, *114*, 4461.

[14] D. Deaven, K. Ho, *Phys. Rev. Lett.* **1995**, *75*, 288.

[15] J. A. Niesse, H. R. Mayne, *J. Chem. Phys.* **1996**, *105*, 4700.

[16] J. Mestres, G. E. Scuseria, *J. Comput. Chem.* **1995**, *16*, 729.

[17] S. Kirkpatrick, M. Vecchi, *Science* **1983**, *220*, 671.

[18] S. Goedecker, *J. Chem. Phys.* **2004**, *120*, 9911.

[19] J. David, J. P. Doye, *J. Phys. Chem. A* **1997**, *101*, 5111.

[20] S. G. Neogi, P. Chaudhury, *J. Comput. Chem.* **2012**, *34*, 471.

[21] S. G. Neogi, P. Chaudhury, *J. Comput. Chem.* **2012**, *33*, 629.

[22] B. Delley, *J. Chem. Phys.* **1990**, *92*, 508.

[23] W. Huang, R. Pal, L.-M. Wang, X. C. Zeng, L.-S. Wang, *J. Chem. Phys.* **2010**, *132*, 054305.

[24] W. Huang, H.-J. Zhai, L.-S. Wang, *J. Am. Chem. Soc.* **2010**, *132*, 4344.

[25] W. Huang, L.-S. Wang, *Phys. Rev. Lett.* **2009**, *102*, 153401.

[26] W. Huang, M. Ji, C.-D. Dong, X. Gu, L.-M. Wang, X. G. Gong, L.-S. Wang, *ACS Nano* **2008**, *2*, 897.

[27] W. Huang, A. P. Sergeeva, H.-J. Zhai, B. B. Averkiev, L.-S. Wang, A. I. Boldyrev, *Nat. Chem.* **2010**, *2*, 202.

[28] H. Do, N. A. Besley, *J. Chem. Phys.* **2012**, *137*, 134106.

[29] H. Do, N. A. Besley, *J. Phys. Chem. A* **2013**, *117*, 5385.

[30] M. J. Frisch, G. W. Trucks, H. B. Schlegel, G. E. Scuseria, M. A. Robb, J. R. Cheeseman, G. Scalmani, V. Barone, B. Mennucci, G. A. Petersson, H. Nakatsuji, M. Caricato, X. Li, H. P. Hratchian, A. F. Izmaylov, J. Bloino, G. Zheng, J. L. Sonnenberg, M. Hada, M. Ehara, K. Toyota, R. Fukuda, J. Hasegawa, M. Ishida, T. Nakajima, Y. Honda, O. Kitao, H. Nakai, T. Vreven, J. A. Montgomery, Jr., J. E. Peralta, F. Ogliaro, M. Bearpark, J. J. Heyd, E. Brothers, K. N. Kudin, V. N. Staroverov, R. Kobayashi, J. Normand, K. Raghavachari, A. Rendell, J. C. Burant, S. S. Iyengar, J. Tomasi, M. Cossi, N. Rega, J. M. Millam, M. Klene, J. E. Knox, J. B. Cross, V. Bakken, C. Adamo, J. Jaramillo, R. Gomperts, R. E. Stratmann, O. Yazyev, A. J. Austin, R. Cammi, C. Pomelli, J. W. Ochterski, R. L. Martin, K. Morokuma, V. G. Zakrzewski, G. A. Voth, P. Salvador, J. J. Dannenberg, S. Dapprich, A. D. Daniels, Ö. Farkas, J. B. Foresman, J. V. Ortiz, J. Cioslowski, D. J. Fox, Gaussian 09, Gaussian, Inc.: Wallingford, CT, **2009**.

[31] S. F. Boys, F. D. Bernardi, *Mol. Phys.* **1970**, *19*, 553.

[32] H.-J. Werner, P. J. Knowles, G. Knizia, F. R. Manby, M. Schütz, *WIREs Comput. Mol. Sci.* **2012**, *2*, 242.

[33] H.-J. Werner, P. J. Knowles, G. Knizia, F. R. Manby, M. Schütz, and others, MOLPRO, version 2010.1, a package of ab initio program, **2010**.

[34] H.-J. Werner, K. Pflüger, *Annu. Rep. Comput. Chem.* **2006**, *2*, 53.

[35] R. Polly, H.-J. Werner, F. R. Manby, P. J. Knowles, *Mol. Phys.* **2004**, *102*, 2311.

[36] S. S. Xantheas, *J. Phys. Chem.* **1996**, *100*, 9703.

[37] X. Xu, W. A. Goddard, *J. Phys. Chem. A* **2004**, *108*, 2305.

[38] J. A. Anderson, G. S. Tschumper, *J. Phys. Chem. A* **2006**, *110*, 7268.

[39] F. Li, L. Wang, J. Zhao, J. R.-H. Xie, K. E. Riley, Z. Chen, *Theor. Chem. Acc.* **2011**, *130*, 341.

[40] S. Grimme, *J. Comput. Chem.* **2004**, *25*, 1463.

[41] S. Grimme, *J. Comput. Chem.* **2006**, *27*, 1787.

[42] M. Schütz, H.-J. Werner, R. Lindh, F. R. Manby, *J. Chem. Phys.* **2004**, *121*, 737.